Constrained Diffusion or Immobile Fraction on Cell Surfaces: A New Interpretation

Toni J. Feder,* Ingrid Brust-Mascher,‡ James P. Slattery,§ Barbara Baird,§ and Watt W. Webb‡
*Department of Physics, ‡School of Applied and Engineering Physics, and §Department of Chemistry, Cornell University, Ithaca, New York 14853

ABSTRACT Protein lateral mobility in cell membranes is generally measured using fluorescence photobleaching recovery (FPR). Since the development of this technique, the data have been interpreted by assuming free Brownian diffusion of cell surface receptors in two dimensions, an interpretation that requires that a subset of the diffusing species remains immobile. The origin of this so-called immobile fraction remains a mystery. In FPR, the motions of thousands of particles are inherently averaged, inevitably masking the details of individual motions. Recently, tracking of individual cell surface receptors has identified several distinct types of motion (Gross and Webb, 1988; Ghosh and Webb, 1988, 1990, 1994; Kusumi et al. 1993; Qian et al. 1991; Slattery, 1995), thereby calling into question the classical interpretation of FPR data as free Brownian motion of a limited mobile fraction. We have measured the motion of fluorescently labeled immunoglobulin E complexed to high affinity receptors ($Fc_\epsilon RI$) on rat basophilic leukemia cells using both single particle tracking and FPR. As in previous studies, our tracking results show that individual receptors may diffuse freely, or may exhibit restricted, time-dependent (anomalous) diffusion. Accordingly, we have analyzed FPR data by a new model to take this varied motion into account, and we show that the immobile fraction may be due to particles moving with the anomalous subdiffusion associated with restricted lateral mobility. Anomalous subdiffusion denotes random molecular motion in which the mean square displacements grow as a power law in time with a fractional positive exponent less than one. These findings call for a new model of cell membrane structure.

INTRODUCTION

According to the fluid mosaic model of Singer and Nicolson (1972), proteins are embedded in a two-dimensional liquid phospholipid bilayer. Both proteins and lipids are free to diffuse rotationally and laterally, limited only by the viscosity of the membrane. The lateral mobility of membrane constituents has been extensively probed by FPR and more recently by single particle tracking (SPT) experiments (for a review see Zhang et al., 1993). It is generally observed that diffusion of proteins in cell membranes is restricted. FPR and SPT techniques have both answered questions and posed new problems (for a recent perspective see Jacobson et al., 1995).

In FPR experiments, a single species on the membrane is labeled with a fluorescent marker, and the fluorophores within some small region are irreversibly photobleached by a short and intense laser pulse. The ensemble averaged mobility of the tracer molecules is characterized by the recovery of fluorescence as unbleached tracer molecules diffuse into the affected region. FPR data are generally interpreted assuming random Brownian diffusion. However, an incomplete fluorescence recovery is usually observed and control experiments have shown that this is not an experimental artifact (Webb et al., 1981).

FPR measurements of lipid and protein diffusion in reconstituted bilayers, and of lipid diffusion in biomembranes, agree with the predictions of hydrodynamic theory (Peters and Cherry, 1982; Saffman and Delbrück, 1975; Vaz et al., 1982). However, in cell membranes, protein lateral self-diffusion coefficients are generally one to three orders of magnitude lower than expected (Kapitza and Jacobson, 1986; Webb et al., 1981). Measured protein diffusion coefficients vary considerably from cell to cell and from one region to another on a single cell. The spread is much wider than expected from the experimental error imposed by the measurements. In addition, most proteins on the cell surface exhibit a substantial immobile subpopulation. These observations suggest heterogeneities in the structure of the membrane. Interactions with the cytoskeleton, cytoplasmic constituents, the extracellular matrix, or with other intramembranous proteins and lipids may account for the constrained diffusion of membrane proteins, but the factors responsible and their relative contributions to hindering protein motion in cell membranes have not been satisfactorily identified.

In contrast to FPR, SPT records the motions of individual particles on the cell surface. A small number of surface elements are labeled with a fluorescent or gold marker, and the trajectories of these labeled proteins or lipids are mapped in time (Gross and Webb, 1988; de Brabander et al., 1991; Ghosh and Webb, 1994; Lee et al., 1993; Qian et al., 1991). This technique has shown that proteins of a single species may exhibit various types of motion: 1) random

Received for publication 7 December 1995 and in final form 21 February 1996.

Toni J. Feder is now at Physics Today Magazine.

Ingrid Brust-Mascher is now at the University of Minnesota.

Address reprint requests to Dr. Watt W. Webb, School of Applied Physics, Cornell University, Clark Hall, Ithaca, New York 14853-2501. Tel: 607-255-3331; Fax: 607-255-7658; E-mail: www2@cornell.edu.

0006-3495/96/06/2767/07 $2.00

Brownian diffusion, 2) directed motion due to active transport (Ghosh, 1991; Kucik et al., 1989; Kusumi et al., 1993; Sheetz et al., 1989) 3) constrained random motion (Anderson et al., 1992; Ghosh, 1991; Ghosh and Webb, 1988, 1990, 1994; Slattery et al., 1991a,b; Kusumi et al., 1993; Slattery, 1995), and 4) immobilization (Ghosh, 1991; Kusumi et al., 1993; Slattery, 1995). A single particle can change its behavior in time. In contrast, lipids diffuse freely in the plasma membrane of spreading and locomoting cells (Lee et al., 1993). To reflect the predominant category of motion observed by SPT, we analyze FPR data with a specific constrained diffusion model denoted anomalous subdiffusion.

This array of behaviors suggests a re-evaluation of the interpretation of FPR data for proteins. Rather than assuming random diffusion with an immobile fraction, the motion might be better characterized by assuming complete but restricted mobility, or anomalous subdiffusion. We first explored this possibility by re-examining conventional diffusion fits to recovery curves simulated assuming anomalous subdiffusion. The fits are as good as fits to experimental photobleaching recovery curves. We also analyzed FPR data according to the anomalous subdiffusion model and found that it fits the data equally well. Both the simulations and fits to experimental data support our hypothesis that the immobile fraction actually arises from the presence of anomalously diffusing particles and suggest that FPR experiments may yield more information if fit with the anomalous subdiffusion model.

THEORY

The mean square displacement of a particle undergoing a random walk is linear in time. In the presence of potential energy traps with binding energies that vary over wide ranges in both space and time, the particle's motion is constrained to anomalous subdiffusion, and the mean square displacement obeys a power law in time (Bouchard and Georges, 1990).

$$\langle r^2 \rangle = \Gamma t^{\alpha} = 4D(t)t \quad \text{with} \quad D(t) = \frac{1}{4}\Gamma t^{\alpha-1}, \qquad (1)$$

where Γ is the transport coefficient, t is time of random walk, and α the time exponent, which gives a measure of the degree to which the motion is restricted. For $\alpha = 1$, this equation reduces to Brownian diffusion with a constant diffusion coefficient, $D = \frac{1}{4}\Gamma$. For $0<\alpha<1$ the motion is time-dependent; on short time scales barriers have little effect, and the particle diffuses freely, but on longer time and length scales, interactions with the barriers become significant, and diffusion is restricted. This fractional power law time dependence of the mean square displacements, designated anomalous subdiffusion, has been found in the theoretical analysis of two dimensional diffusion only with the constraints on the potential energy traps specified above (Bouchard and Georges, 1990). Particles whose motion is thus constrained are hypothesized to contribute to the apparent immobile fraction in the conventional interpretation of FPR data.

To test this hypothesis we altered the equation used to fit FPR data. Following Axelrod et al. (1976), we solved the diffusion equation, which was modified to allow for the time-dependence of Eq. 1 and an immobile fraction. For a Gaussian beam, fluorescence recovery is given by

$$F(t) = \left\{ F^0 \sum_{n=1}^{\infty} \frac{(-\kappa)^n}{n!} \frac{1}{1 + n(1 + 2(t/\tau)^{\alpha})} \right\} R + (1 - R)F_0. \qquad (2)$$

F^0 is the fluorescence intensity before bleaching; F_0 is the fluorescence intensity immediately after bleaching; the parameter κ is related to the bleach depth; R is the mobile fraction; and τ is the characteristic time, defined in terms of the transport coefficient Γ, the beam radius ω, and α by $\tau = (\omega^2/\Gamma)^{1/\alpha}$.

The series solution in Eq. 2 can be approximated by

$$F(t) = \frac{F_0 + F_{\infty}\left(\frac{t}{t_{1/2}}\right)^{\alpha}}{1 + \left(\frac{t}{t_{1/2}}\right)^{\alpha}}, \qquad (3)$$

with the mobile fraction given by

$$R = \frac{F_{\infty} - F_0}{F^0 - F_0}. \qquad (4)$$

F_{∞} is the fluorescence intensity as $t \to \infty$, and $t_{1/2}$ is the half time for recovery, related to the characteristic time τ in Eq. 2 by $t_{1/2} = \beta\tau$. β is an empirical parameter ($1<\beta<2$) that depends on the bleach depth (Yguerabide et al., 1982). The recovery is given by Eq. 4, and is complete if $R = 1$.

To check the validity of this approximation we simulated curves with Eq. 2 and fit them using Eq. 3. For bleach depths up to 70%, values of $F(t)$ differ by <1% and values of α by <3%. Eq. 2 and 3, with 4, reduce to Brownian diffusion or anomalous subdiffusion, depending on the parameters α and R. The motion corresponds to Brownian diffusion if $\alpha = 1$ and to anomalous diffusion if $\alpha<1$.

The mobile fraction is introduced in the recovery curves by expressing F_{∞} in terms of R in Eq. 4, and substituting into Eq. 3:

$$F(t) = \frac{F_0 + (R(F^0 - F_0) + F_0)\left(\frac{t}{t_{1/2}}\right)^{\alpha}}{1 + \left(\frac{t}{t_{1/2}}\right)^{\alpha}}. \qquad (5)$$

Simulations

To determine how well the usual analysis of FPR data, i.e., diffusion with an immobile fraction, can fit anomalous subdiffusion, we simulated recovery curves using Eq. 2 with

$R = 1$ and a range of α values, and fit these curves with Eq. 3, fixing $\alpha = 1$ (Fig. 1). The simulations go to $t = 10\tau$, approximating our FPR experiments. For $\alpha = 1$, the simulation reduces to random Brownian diffusion, and the fit is as good as the approximation to the full series solution. For $0<\alpha<1$, the fits are still close enough that both curves could fit FPR data. The symmetric case of fitting simulated Brownian diffusion recovery curves (Eq. 2, with $\alpha = 1$) by anomalous subdiffusion (Eq. 3, with $F_\infty = F^0$) also suggests that either interpretation could be applied to FPR data (not shown). The smaller the exponent α in the simulations, the larger the immobile fraction $1-R$ obtained from the fit. Fig. 5 illustrates this anti-correlation for the simulations, and for the analysis of actual FPR data, discussed below.

METHODS

Rat basophilic leukemia cells (RBL-2H3) were grown and harvested as described in Barsumian et al. (1981). They were plated on coverslips for two days, forming a confluent monolayer of flat cells. Low density lipoprotein (LDL) particles labeled with the fluorescent lipid analogue 1,1′-dioctadecyl-3,3,3′,3′-tetramethylindo-carbocyanine (dil) were covalently coupled to murine immunoglobulin E (IgE) to form bright, fluorescent monomeric dil-LDL-IgE (Kulcyzcki and Metzger, 1974; Slattery, 1995). These dil-LDL-IgE bind with high affinity (essentially irreversibly) to the $Fc_\epsilon RI$ receptors for IgE on the surface of RBL cells (Kulcyzcki and Metzger, 1974; Slattery, 1995). For SPT experiments, a few hundred IgE receptors (<0.1%) were labeled. The label is uniformly dispersed and, therefore, probes receptor behavior over the entire unattached cell surface. For most FPR experiments, cells attached to coverslips were sensitized overnight with a tenfold molar excess of fluorescein-5′-isothiocyanate-IgE (FITC-IgE) and then washed before measurements (Erickson et al., 1986). For a few FPR experiments, cells were incubated with dil-LDL-IgE in suspension, washed, and freshly plated for each experiment.

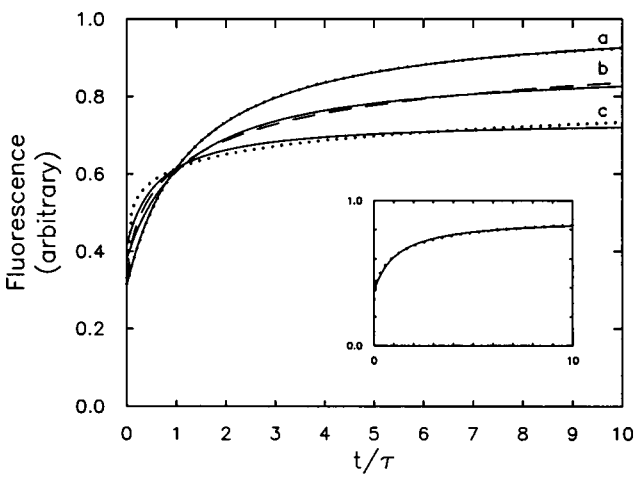

FIGURE 1 Simulated recovery curves and fits. Simulated anomalous subdiffusion curves (*broken lines*, Eq. 2 with $R = 1$ and a range of α values) were fit by Brownian diffusion with an immobile fraction (*solid lines*, Eq. 3 with $\alpha = 1$). The bleach depth was set as 0.3, a typical experimental value. The values used for α and those obtained for R are: $\alpha = 1$, $R = 101\%$ (*a*); $\alpha = 0.6$, $R = 81\%$ (*b*); $\alpha = 0.3$, $R = 55\%$ (*c*). *Inset*: Best fit (*solid line*) to the average of the three simulated curves (*broken line*) gives $R = 80\%$.

FPR measurements were performed as described in Thomas and Webb (1990) using the 488-nm line of a Coherent Innova 90 argon ion laser (Santa Clara, CA) as the source for both bleaching and monitoring fluorescence recovery. The spot radius was measured from its pre-bleach fluorescence images taken on the cell with a sensitive charge-coupled device camera. Photobleaching due to the monitor beam was less than 5%.

SPT experiments were performed as described in Ghosh and Webb (1994) and Slattery (1995); 150 fluorescence images, each an average over 1.6 s, were acquired over a total of 4 min for each data run. An automated tracking routine identified particles with a precision of 30 nm by calculating the intensity weighted mean pixel location in the n^{th} image and then locating and identifying the particles from the $n-1^{th}$ image (Ghosh and Webb, 1994). The mean square displacement $\langle(\Delta r)^2\rangle$ was calculated from the trajectories for nonoverlapping time steps Δt and fit to Eq. 1.

RESULTS

Results of FPR and tracking experiments performed on fluorescently labeled IgE complexed with high affinity receptors (IgE-$Fc_\epsilon RI$) on the surface of RBL cells (Erickson et al., 1986) using either FITC-IgE or dil-LDL-IgE are reported here.

Single particle tracking

Individual dil-LDL-IgE-$Fc_\epsilon RI$ on RBL cells were tracked automatically by time-lapse fluorescence video microscopy (Ghosh and Webb, 1994; Slattery, 1995). The mean square displacement (Eq. 1) was calculated for each trajectory and the exponent α was used to characterize the motion. In our sample of 241 tracked receptors, we found that 10% exhibited Brownian motion ($0.9<\alpha<1.1$), 56% anomalous subdiffusion ($0.1<\alpha<0.9$), 7% directed motion ($\alpha>1.1$), and 27% of receptors were found to have $0<\alpha<0.1$, which we define as immobile. The average time exponent for all mobile particles ($\alpha>0.1$) is $\alpha = 0.64 \pm 0.45$. The diffusion coefficient is time-dependent; using Eq. 1 we obtained its value at 1 s ($\Gamma/4$) and used it for comparisons between particles. For all particles with $\alpha>0.1$ the average is $D(1s) = 0.96 \pm 0.4\times10^{-10}$ cm^2/s.

FPR experiments

Most FPR experiments were performed with FITC-IgE-$Fc_\epsilon RI$. The quality of the diffusion fits to simulations of anomalous subdiffusion (Fig. 1) suggests that the conventional interpretation of FPR data may not be the best. We therefore fit our data to different models, using Eq. 3 with different sets of parameters: 1) The standard model assuming Brownian diffusion ($\alpha = 1$) with an immobile fraction, and F_0, F_∞, $t_{1/2}$ are the fit parameters; 2) The anomalous subdiffusion model, in which complete recovery is ensured by fixing F_∞ to the prebleach value F^0, and the fit parameters are α, F_0, and $t_{1/2}$; 3) A more general model, which includes anomalous subdiffusion and an immobile fraction by allowing both α and R to vary; in this case there are four free parameters: α, F_0, F_∞, and $t_{1/2}$.

Fig. 2 shows an experimental recovery curve for monomeric FITC-IgE-$Fc_\epsilon RI$ on an RBL cell with the best fits to

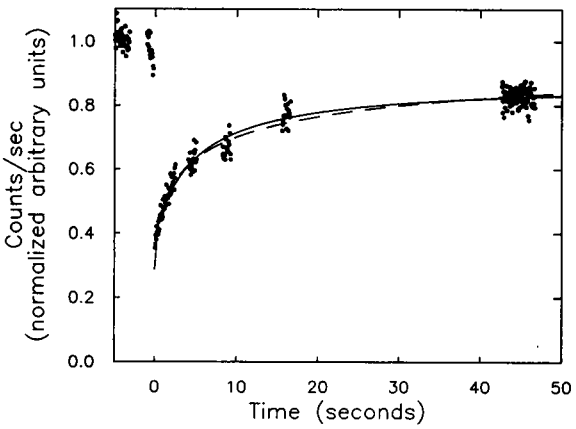

FIGURE 2 FPR recovery curve and fits for FITC-IgE-Fc$_\epsilon$RI. Monolayer RBL cells were sensitized overnight with FITC-IgE. The vertical axis is counts per second, normalized to the prebleach intensity. Points present a set of experimental data. Fits to pure diffusion with an immobile fraction (*solid line*; $R = 79\%$, $D = 5\times10^{-10}$ cm^2/s, $t_{1/2} = 4.9$ s) and to anomalous subdiffusion (*dashed line*; $\alpha = 0.6$, $D(1\text{ s}) = 10\times10^{-10}$ cm^2/s, $t_{1/2} = 5.7$ s) are shown.

the two limiting models: Brownian diffusion with an immobile fraction and anomalous subdiffusion with complete recovery. The two fits cannot be distinguished by χ^2, the parameter minimized in the fitting program. Plotting the data in logarithmic time, however, accentuates the difference at early times, and in many cases the anomalous subdiffusion model appears to be better (For example, see Fig. 3.). To test whether longer observation times would distinguish the two models, we added to the experimental data an artificial set of points that falls on the anomalous subdiffusion fit curve. The set comprising the experimental data and added points was then fit with both models. The two fits deviate at early and late times (Fig. 3), suggesting that longer observation times (~10 times longer) could distinguish between the two models. However, the limitations imposed by photobleaching and instrument stability make long periods of data acquisition impractical.

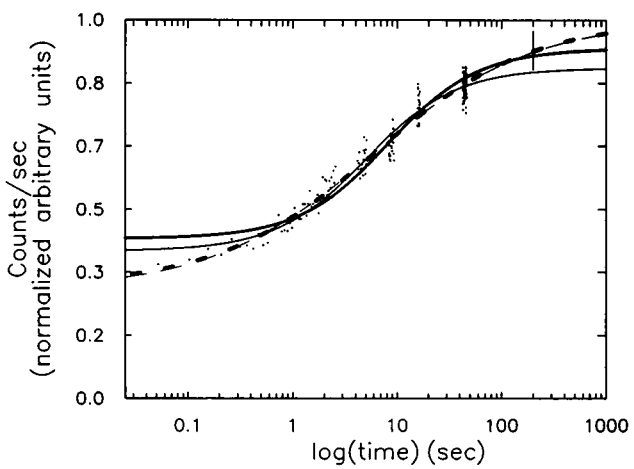

FIGURE 3 Long time extension of data. The Brownian diffusion plus immobile fraction model and anomalous subdiffusion model could be distinguished with much longer times of data acquisition. The data (*points*) were fit by each model in logarithmic time (*thin solid line*, Brownian diffusion; *thin broken line*, anomalous subdiffusion). An additional set of points was calculated to fall on the anomalous subdiffusion curve at a later time with uncertainties of the same order as the experimental data (*line segment*). The experimental data with the added points were then fit by the two models. The resulting fits (*thick solid line*, Brownian diffusion; *thick dashed line*, anomalous diffusion) show that the two models diverge at both early and late times.

Because tracking data indicate that a non-negligible fraction of particles is immobile ($\alpha \sim 0$) on the time and length scales of our FPR experiments, we analyzed our FPR data ($n = 158$) with four fitting parameters, allowing for both anomalous subdiffusion and an immobile fraction (Eq. 3). In some cases this fitting method reduces to pure diffusion with an immobile fraction (~8%), in others anomalous subdiffusion is favored (~28%), and in some others (~43%) the resulting values lie between those of the two limiting models; both R and α are larger than obtained by the respective 3-parameter fits, but they are smaller than one, suggesting the presence of both immobile particles and particles with constrained mobility. In the remaining cases the four-parameter fit gives results that are difficult to interpret physically; either the mobile fraction exceeds 100%, or α gets very large. The parameters from 158 recovery curves for all three models are summarized in Table 1.

A few FPR experiments were performed with dil-LDL-IgE to permit a direct comparison with the tracking data. Fig. 4 shows a sample recovery curve with the fits to the two limiting models. As seen in this example, R from the standard model and α from the anomalous subdiffusion model are very small, indicating that the motion is very restricted. But even in this case with very low mobility, both models fit the data. The fitting parameters are summarized in Table 2. The low mobility observed with dil-LDL-IgE-Fc$_\epsilon$RI is probably due to interactions of the bulky dil-LDL label with the extracellular matrix (Slattery, 1995).

DISCUSSION

SPT experiments have shown that a single species of protein on the cell surface exhibits different types of motion. LDL receptors on fibroblasts exhibit Brownian diffusion, anomalous subdiffusion, directed motion and correlated motion, in which many receptors move in parallel (Ghosh and Webb, 1988; 1990; 1994). Most diffusing particles exhibit anomalous subdiffusion with a transport coefficient consistent with the diffusion coefficients measured by pattern FPR experiments (Barak and Webb, 1982). The detailed description of cell surface mobility obtained suggested that the apparent immobile fraction measured by FPR experiments could be explained by particles exhibiting anomalous subdiffusion. Our experiments support this hypothesis.

TABLE 1 Fitting parameters from FPR data for FITC-IgE-Fc$_\epsilon$RI. The parameters obtained from fitting FPR data on FITC-IgE-Fc$_\epsilon$RI on RBL cells using the conventional interpretation of diffusion with an immobile fraction (Eq. 3 with $\alpha = 1$), complete anomalous subdiffusion (Eq. 3 with $R = 1$), and a four parameter fit allowing for anomalous subdiffusion and an immobile fraction are summarized in this table. Data were taken on three different days. These diffusion coefficients are somewhat higher than is typical because of extended plating times. Errors are standard deviations. Comparison of D(50 s) with D(1 s) illustrates the slowing of effective diffusivity with observation time scales.

Model	R%	D ($\times 10^{-9}$ cm^2/s)	α	D(1 s) ($\times 10^{-9}$ cm^2/s)	D(50 s) ($\times 10^{-9}$ cm^2/s)
Diffusion with immobile fraction (n = 158)	77 ± 15	1.3 ± 1.0			
Anomalous sub-diffusion (n = 151)			0.46 ± 0.22	3.0 ± 2.6	0.29 ± 0.17
Anomalous subdiffusion with immobile fraction (n = 126)	89 ± 13		0.61 ± 0.22	3.6 ± 3.2	0.71 ± 0.62

Simulations and FPR experiments

Simulations show that a model assuming Brownian diffusion modified by an immobile fraction can approximately fit an anomalous subdiffusion recovery curve over the usual time scale of an FPR experiment. FPR measurements on IgE-Fc$_\epsilon$RI on RBL cells can be fit equally well by both models. This supports the hypothesis that the immobile fraction includes particles diffusing anomalously and suggests that FPR data for proteins be analyzed differently. The mobility of a lipid analog is better fit by the pure diffusion model (not shown), in agreement with Lee et al.'s observation by SPT that lipids diffuse freely in the plasma membrane (Lee et al., 1993).

SPT experiments have shown that some particles are immobile ($\alpha \sim 0$) over the duration of the experiment. Thus, the best fit to FPR data appears to be a four-parameter fit, which allows both anomalously diffusing and immobile particles. However, our fits to the two limiting models show that α and $(1-R)$ can substitute for each other. As illustrated in Fig. 5, the constraints of these two models result in an anticorrelation between the immobile fraction and α for both simulated and experimental data. The four-parameter fit is thus sensitive to the initial estimates. Therefore, it is probably best to fit FPR data with the two limiting models and obtain lower estimates for both α and R.

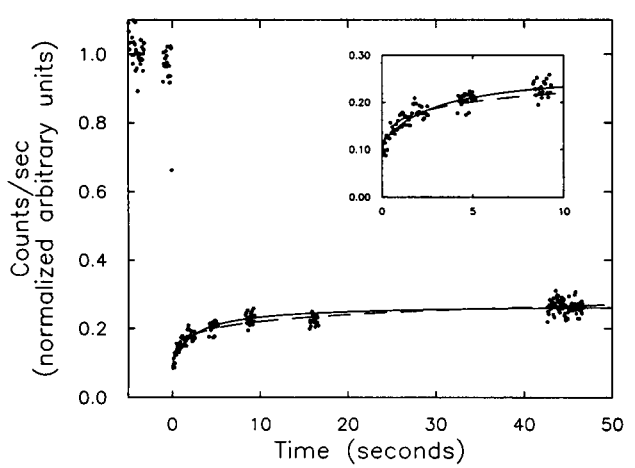

FIGURE 4 FPR recovery curve and fits for dil-LDL-IgE-Fc$_\epsilon$RI. RBL cells in suspension were incubated with dil-LDL-IgE and plated for each experiment. The vertical axis is counts per second, normalized to the prebleach intensity. Points represent experimental data. Fits to pure diffusion with an immobile fraction (*solid line*; R = 18%, $D = 8.4\times10^{-10}$ cm^2/s, $t_{1/2}$ = 3.0 s) and to anomalous subdiffusion (*dashed line*; α = 0.17, D(1 s) = 0.71×10^{-10} cm^2/s, $t_{1/2}$ = 20174 s) are shown.

Comparison between FPR and SPT data

FPR and SPT measurements can be compared by simulating FPR recovery curves from SPT data using Eq. 5. Values for R, α, and $t_{1/2} = \beta(\{[\omega]^2/\Gamma\})^{1/\alpha}$, can be calculated as averages of the values obtained from individually tracked molecules. We simulated recovery curves from Eq. 5 using a wide range of values for α and R. Both fitting models, diffusion with an immobile fraction and anomalous subdiffusion, are remarkably insensitive to the values used to generate the recovery curves: fits were good for $0.1<\alpha\leq1$ and for $20\%\leq R\leq100\%$.

We compared SPT and FPR data for dil-LDL-IgE-Fc$_\epsilon$RI. The average α, R, and D(1 s) calculated for all mobile particles ($\alpha>0.1$), were used to construct a recovery curve using Eq. 5. This curve was then fit by the two limiting models (Fig. 6). In the time scale of an FPR experiment (~50 s), the composite curve has a low recovery, giving a small mobile fraction and a small α consistent with FPR measurements. As expected, the values obtained are lower than the values used for the simulation, because only one parameter, either α or R, is used in the fit and is compensating for the presence of both in the membrane as observed for FPR data.

Model

The array of observed behaviors may be explained by a dynamic membrane structure. Anomalous subdiffusion can occur in a random array of continously changing potential energy traps, whose range of binding energies and thus of escape rates is large so that there is no average binding time (Bouchard and Georges, 1990). This "infrastructure," varying both in time and space, could be created by complexes of membrane proteins and lipids, cytoskeletal elements, and

TABLE 2 Fitting parameters from FPR data for dil-LDL-IgE-Fc$_\epsilon$RI. The parameters obtained from fitting FPR data on dil-LDL-IgE-Fc$_\epsilon$RI on RBL cells using the conventional interpretation of diffusion with an immobile fraction (Eq. 3 with $\alpha = 1$), and complete mobility with anomalous subdiffusion (Eq. 3 with $R = 1$) are summarized in this table. Errors are standard deviations. D(1 s) and D(50 s) are compared as described in Table 1.

Model	R%	D ($\times 10^{-10}$ cm^2/s)	α	D(1 s) ($\times 10^{-10}$ cm^2/s)	D(50 s) ($\times 10^{-14}$ cm^2/s)
Diffusion with immobile fraction (n = 11)	21 ± 11	10.0 ± 7.9			
Anomalous subdiffusion (n = 11)			0.15 ± 0.07	1.4 ± 1.1	5.7 ± 5.6

extracellular matrix components. Interactions of a diffusing molecule with such a dynamic infrastructure would vary, resulting in both selective and nonspecific, time-dependent constraints. If the interaction is sufficiently strong to prevent escape over the time scale of the experiment, immobilization occurs.

This model can also explain other experimental results. Edidin and Stroynowski (1990) observed an increase in D and a decrease in R with increasing bleaching radius in their FPR measurements on a transmembrane protein (but not on a lipid-linked protein with the same extracellular domain) in transfected mouse hepatoma cells. They inferred membrane domains on the scale of microns. Kusumi et al. (1993) performed FPR and SPT measurements on E-cadherin, epidermal growth factor receptor, and transferrin receptor in a cultured mouse keratinocyte cell line. Comparing the immobile fraction obtained by FPR with the number of immobile and constrained particles obtained by SPT, they concluded that the plasma membrane is compartmentalized into many small domains (300–600 nm), and that receptors can sometimes move between them. Alternatively, all these observations may be explained by interactions with a random array of traps, resulting in restricted, time-dependent motion on all observable spatial scales. The corresponding range of trapping times in anomalous subdiffusion would cover the accessible experimental range from ~0.1 s to ~10^3 s. The application of a pure diffusion model to time-dependent motion can lead to distorted interpretations, in which both the diffusion coefficient and the mobile fraction depend on the time and length scale of the experiment (Nagle, 1992).

CONCLUSIONS

Simulations and analysis of FPR data for IgE-Fc$_\epsilon$RI on RBL cell surfaces show that the traditional interpretation, in which Brownian diffusion and an immobile subpopulation are assumed, and a new model, in which complete but restricted mobility is allowed, fit FPR measurements

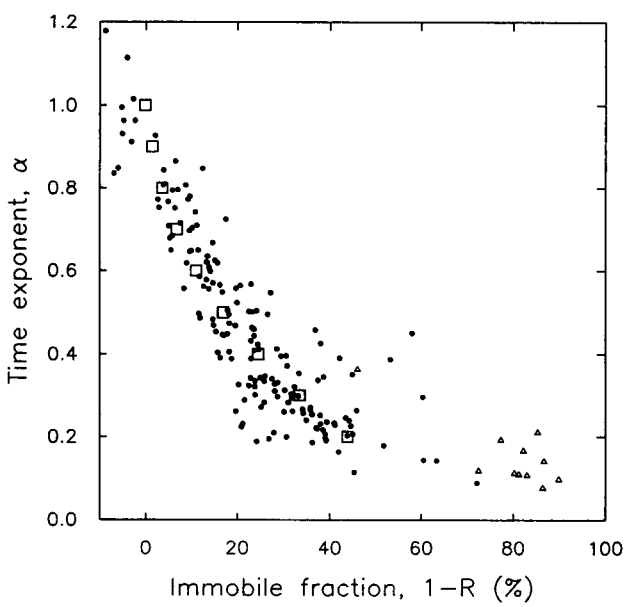

FIGURE 5 Time exponent versus immobile fraction. Open squares correspond to simulated data of the type shown in Fig. 1, points are from fits to 163 photobleach recovery curves of FITC-IgE and triangles from 11 recovery curves of dil-LDL-IgE. The simulations were made with typical FPR values for the observation time ($t = 10\tau$) and bleach depth (64%); the position and slope of the theoretical curve is sensitive to these parameters, but the general trend is not affected.

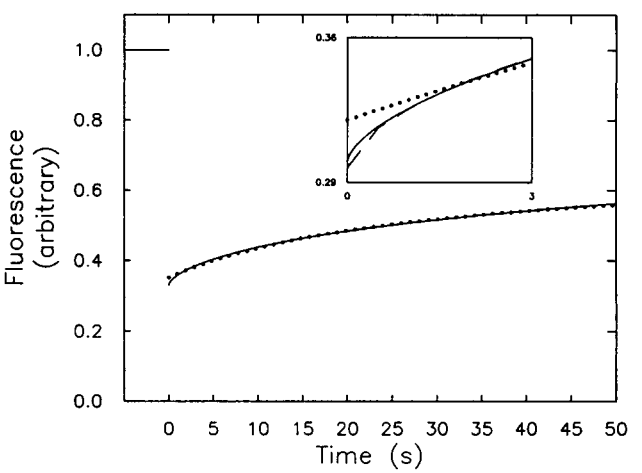

FIGURE 6 Composite recovery curve from individual particle trajectories. An equivalent FPR recovery curve (*solid line*) was simulated from Eq. 5, using the mean values R = 73%, α = 0.64 and D(1 s) = 0.96×10^{-10} cm^2/s, obtained from tracking individual dil-LDL-IgE-Fc$_\epsilon$RI on RBL cells (Slattery, 1995). The bleach depth and bleaching spot radius were chosen to correspond to typical experimental values. The dotted line is the best fit using the anomalous subdiffusion model, giving α = 0.57, D(1 s) = 0.33×10^{-10} cm^2/s, and $t_{1/2}$ = 288 s. The dashed line is the best fit assuming Brownian motion, with R = 38%, D = 1.0×10^{-10} cm^2/s, and $t_{1/2}$ = 29 s.

equally well. FPR inherently averages over a large number of particles, that, as shown by SPT, exhibit different behaviors, including constrained diffusion and immobilization. As discussed above, a four-parameter fit allowing both immobile and anomalously diffusing particles, though theoretically better, is not practical. It appears best to fit FPR with the two limiting models to obtain lower limits for the values of both R and α. FPR experiments can be used for comparisons of cell surface mobility under different conditions, as long as fixed observation times and distance scales are used. Detailed studies of receptor motion require tracking of individual receptors.

This research was supported by National Institutes of Health grants P41RR04224 and AI10306, and National Science Foundation grants DIR8800278 and GER9023463; and was carried out in the National Institutes of Health-National Science Foundation Developmental Resource for Biophysical Imaging and Optoelectronics. The authors thank Dr. David Holowka for helpful comments. The first two authors contributed equally to this work.

REFERENCES

Anderson, C. M., G. N. Georgiou, I. E. G. Morrison, G. V. W. Stevenson, and R. J. Cherry. 1992. Tracking of cell surface receptors by fluorescence digital imaging microscopy using a charge-coupled device camera. *J. Cell Sci.* 101:415–425.

Axelrod, D., D. E. Koppel, J. Schlessinger, E. Elson, and W. W. Webb. 1976. Mobility measurement by analysis of fluorescence photobleaching recovery kinetics. *Biophys. J.* 16:1055–1069.

Barak, L. S., and W. W. Webb. 1982. Diffusion of low density lipoprotein-receptor complex on human fibroblasts. *J. Cell Biol.* 95:846–852.

Barsumian, E. L., C. Isersky, M. K. G. Petrino, and R. P. Sirganian. 1981. IgE induced histamine release from rat basophilic leukemia cell lines: isolation of releasing and non-releasing doses. *Eur. J. Immunol.* 11: 317–323.

J-P. Bouchaud, and A. Georges. 1990. Anomalous diffusion in disordered media: statistical mechanisms, models and physical applications. *Phys. Rep.* 195:127–293.

de Brabander, M., R. Huydens, A. Ishihara, B. Holifield, K. Jacobson, and H. Geerts. 1991. Lateral diffusion and retrograde movements of individual cell surface components on single motile cells observed with nanovid microscopy. *J. Cell Biol.* 112:111–124.

Edidin, M., and I. Stroynowski. 1990. Differences between the lateral organization of conventional and inositol phospholipid-anchored membrane proteins. A further definition of micrometer scale membrane domains. *J. Cell Biol.* 112:1143–1150.

Erickson, J., P. Kane, B. Goldstein, D. Holowka, and B. Baird. 1986. Cross-linking of IgE-receptor complexes at the cell surface: a fluorescence method for studying the binding of monovalent and bivalent haptens to IgE. *Mol. Immunol.* 23:769–781.

Ghosh, R. N. 1991. Mobility and clustering of individual low density lipoprotein receptor molecules on the surface of human skin fibroblasts. PhD thesis. Cornell University, Ithaca, New York. 260 pp.

Ghosh, R. N., and W. W. Webb. 1988. Results of automated tracking of low density lipoprotein receptors on cell surfaces. *Biophys. J.* 53:352a.

Ghosh, R. N., and W. W. Webb. 1990. Evidence for intra-membranous constraints to cell surface low density lipoprotein receptor motion. *Biophys. J.* 57:286a.

Ghosh, R. N., and W. W. Webb. 1994. Automated detection and tracking of individual and clustered cell surface low density lipoprotein receptor molecules. *Biophys. J.* 66:1301–1318.

Gross, D., and W. W. Webb. 1988. Cell surface clustering and mobility of the liganded LDL receptor measured by digital video fluorescence microscopy. *In* Spectroscopic Membrane Probes, Vol II. Leslie M. Loew, editor. CRC Press, Inc., Boca Raton, FL. 19–45.

Jacobson, K., E. D. Sheets, and R. Simon. 1995. Revisiting the fluid mosaic model of membranes. *Science.* 268:1441–1442.

Kapitza, H. G., and K. Jacobson. 1986. Lateral motion of membrane proteins. *In* Techniques for the Analysis of Membrane Proteins. C. J. Ragan and R. J. Cherry, editors. Chapman and Hall, London. 345–375.

Kucik, D. F., E. L. Elson, and M. P. Sheetz. 1989. Forward transport of glycoproteins on leading lamellipodia in locomoting cells. *Nature.* 340: 315–317.

Kulcyzcki, A., and H. Metzger. 1974. The interaction of IgE with rat basophilic leukemia cells. II. Quantitative aspects of the binding reaction. *J. Exp. Med.* 140:1676–1695.

Kusumi, A., Y. Sako, and M. Yamamoto. 1993. Confined lateral diffusion of membrane receptors as studied by single particle tracking (nanovid microscopy). Effects of calcium-induced differentiation in cultured epithelial cells. *Biophys. J.* 65:2021–2040.

Lee, G. M., F. Zhang, A. Ishihara, C. L. McNeil, and K. A. Jacobson. 1993. Unconfined lateral diffusion and an estimate of pericellular matrix viscosity revealed by measuring the mobility of gold-tagged lipids. *J. Cell Biol.* 120:25–35.

Nagle, J. F. 1992. Long tail kinetics in biophysics? *Biophys. J.* 63: 366–370.

Peters, R., and R. J. Cherry. 1982. Lateral and rotational diffusion of bacteriorhodopsin in lipid bilayers: experimental test of the Saffman-Delbrück equations. *Proc. Nat. Acad. Sci. USA.* 79:4317–4321.

Qian, H., M. P. Sheetz, and E. L. Elson. 1991. Single particle tracking: analysis of diffusion and flow in two dimensional systems. *Biophys. J.* 60:910–921.

Saffman, P. G., and M. Delbrück. 1975. Brownian motion in biological membranes. *Proc. Nat. Acad. Sci. USA.* 72(8):3111–3113.

Sheetz, M. P., S. Turney, H. Qian, and E. L. Elson. 1989. Nanometre-level analysis demonstrates that lipid flow does not drive membrane glycoprotein movements. *Nature.* 340:284–288.

Singer, S. J., and G. L. Nicolson. 1972. The fluid mosaic model of the structure of cell membranes. *Science.* 175:721–731.

Slattery, J. P. 1995. Lateral mobility of $Fc_{\epsilon}RI$ on rat basophilic leukemia cells as measured by single particle tracking using a novel bright fluorescent probe. Ph. D. thesis. Cornell University, Ithaca, New York. 153 pp.

Slattery, J. P., D. Holowka, R. Ghosh, W. W. Webb, and B. Baird. 1991a. Bright fluorescent probe for high precision tracking of individual immunoglobulin E receptor molecules. *Biophys. J.* 59:384a.

Slattery, J. P., D. Holowka, R. Ghosh, W. W. Webb, and B. Baird. 1991b. Precision Cell Surface Tracking of Individual Immunoglobulin E Receptor Molecules with a Bright Fluorescent Probe. XV Congress of the International Society for Analytical Cytology, The Grieghallen, Bergen, Norway, 25–30

Thomas, J. L., and W. W. Webb. 1990. Fluorescence photobleaching recovery: a probe of membrane dynamics. *In* Noninvasive Techniques in Cell Biology. S. Ginstein and K. Foskett, editors. Wiley-Liss, New York. 129–152.

Vaz, W. L. C., M. Criado, V. M. C. Madeira, G. Schoellmann, and T. M. Jovin. 1982. Size dependence of the translational diffusion of large integral membrane proteins in liquid-crystalline phase lipid bilayers: a study using fluorescence recovery after photobleaching. *Biochem.* 21: 5608–5612.

Webb, W. W., L. S. Barak, D. W. Tank, and E-S. Wu. 1981. Molecular mobility on the cell surface. *Biochem. Soc. Symp.* 46:191–205.

Yguerabide, J., J. A. Schmidt, and E. E. Yguerabide. 1982. Lateral mobility in membranes as detected by fluorescence recovery after photobleaching. *Biophys. J.* 39:69–75.

Zhang, F., G. M. Lee, and K. Jacobson. 1993. Protein lateral mobility as a reflection of membrane microstructure. *BioEssays* 15:579–588.